PERFORMANCE REVIEW -- NEUTRON HODOSCOPE AT TREAT

G. S. Stanford, A. DeVolpi, C. L. Fink,
J. P. Regis, E. A. Rhodes, and R. R. Stewart

Reactor Analysis and Safety Division
Argonne National Laboratory
Argonne, Illinois 60439

ABSTRACT

The current fuel-motion-detection capabilities of the neutron hodoscopes at TREAT are outlined and discussed, including such topics as spatial and fuel-density resolution, dynamic range, and corrections for detector dead time and supralinearity. Capabilities and analytical techniques are illustrated with examples from several of the power-transient experiments that have been run in the TREAT reactor.

INTRODUCTION

The original ANL fast-neutron hodoscope has been producing fuel-motion data for test transients at the TREAT reactor since 1965, at first with a limited complement of 50 channels, expanded in 1969 to a capability for 334 channels.[1,9] Each operational channel contains a neutron detector behind a collimating slot in a steel block, arranged as shown in Figs. 1 and 2. The operational field of view of the original ("51-cm") hodoscope is approximately 470 mm tall by 50 mm wide at the test element--adequate to encompass a 7-pin bundle of test fuel with a height of 343 mm (13.5 in). Recently the 51-cm collimator was removed from the north face of TREAT (to be installed soon at the south face), and at the north face was installed a new ("122-cm") collimator[2] with a viewing area 1220 mm tall, to accommodate 914-mm (36 in.) fuel pins. The instrumented width of the viewing area for neutron detection is 33 mm at present, and slots are provided to double that width if the need arises. For the remainder of this report, all remarks will apply to the original collimator, unless otherwise stated.

SPATIAL RESOLUTION

The term "spatial resolution," as applied to an instrument like the hodoscope, is susceptible to a number of differing definitions: (1) In the traditional meaning of "resolving power" as used in optics, implying the ability to distinguish a dip between two peaks, the resolving power of the hodoscope is equal to twice the interchannel distance. In this sense, for the 51-cm collimator the spatial resolving power is 7.2 mm horizontally and 45 mm vertically (see Table 1, which gives some of the important dimensions for both the 51-cm collimator and the 122-cm collimator). (2) The spatial resolution of the hodoscope can be considered to be the FWHM of the response function of a single channel. In this case, the resolving power

BLANK PAGE

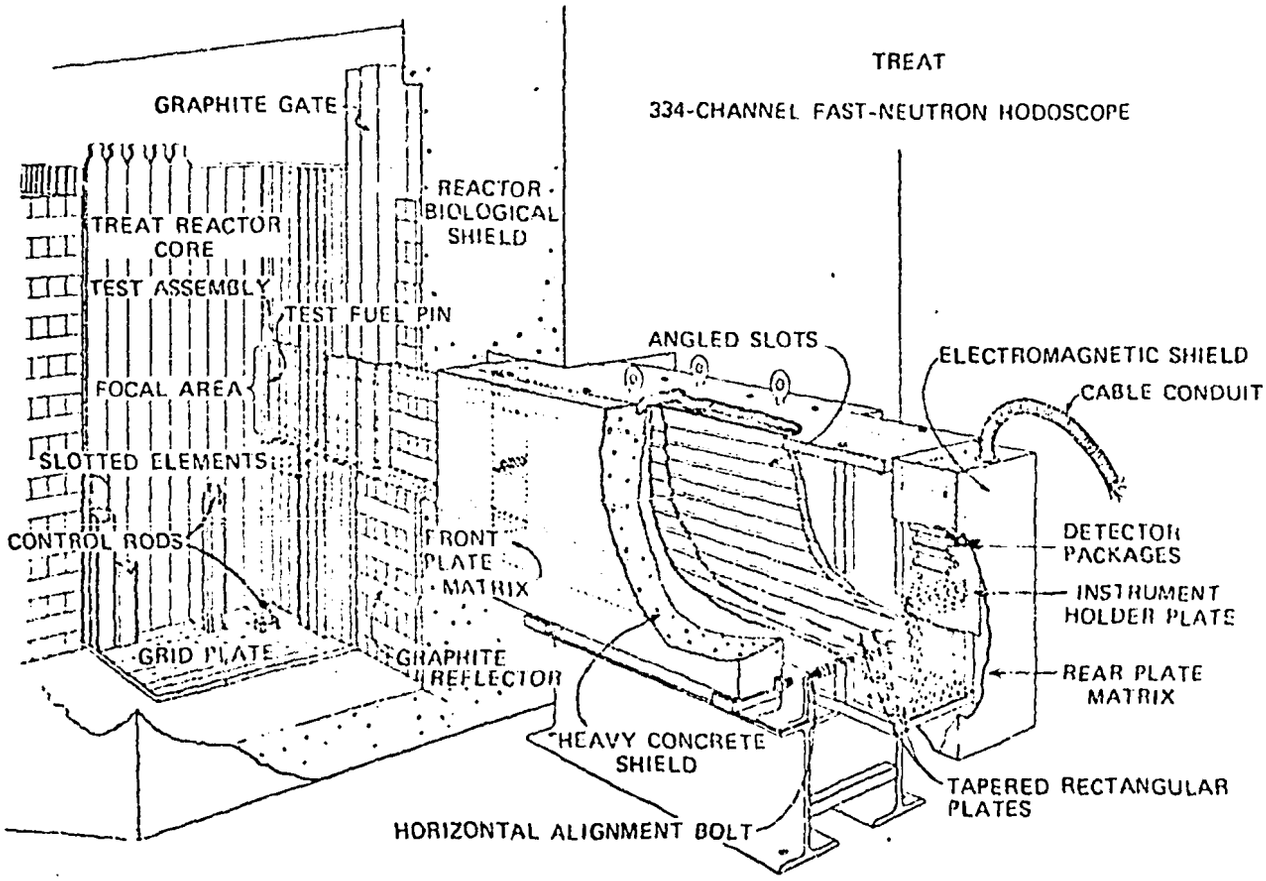

Fig. 1. Cutaway view of fast-neutron hodoscope collimator situated at north face of TREAT reactor.

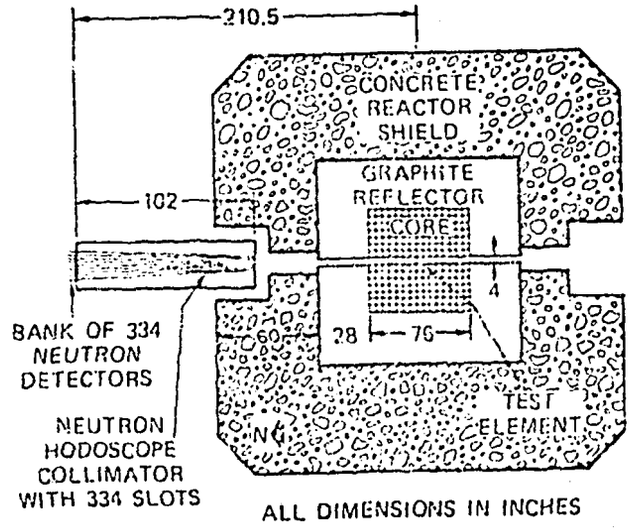

Fig. 2. Schematic plan view of relationship between hodoscope collimator and TREAT core.

TABLE 1. COLLIMATOR DATA

	Collimator	
	51-cm	122-cm
Channel size		
Vertical	14.4 mm	8.9 mm
Horizontal	2.4 mm	2.4 mm
Channel separation at reactor center		
Vertical	22.5 mm	34.5 mm
Horizontal	3.6 mm	6.6 mm
Rows of channels		
Total	23	36
Instrumented for neutrons	21	36
Columns of channels		
Total	15	10
Instrumented for neutrons	13	5
Field of view (maximum)		
Vertical	510 mm	1220 mm
Horizontal	57 mm	66 mm
Collimator		
Length	2.59 mm	1.81 m
Distance from reactor center	2.79 m	2.46 m
Motion resolution (see text)		
Vertical	2 mm	5 mm (est.)
Horizontal	0.2 mm	0.5 mm (est.)
Mass: good conditions	0.4 g	1 g (est.)
best conditions	0.05 g	0.1 g (est.)

of the 51-cm hodoscope is approximately equal to the channel separation: 3.6 mm horizontally and 22.5 mm vertically. We choose to call this the "static resolution" of the hodoscope. (3) The primary purpose of the hodoscope, however, is to analyze for displacements of test fuel, so that the ability to identify the motion of small amounts of fuel--or, equivalently, the small movements of large amounts of test fuel--is important. Under good conditions, counting-rate changes of 5% or less can be both statistically significant and otherwise credible. One way for such a change to arise is for the edge of a region of fuel to be displaced by a small amount. With the 51-cm hodoscope, displacements of intact fuel pellets by as little as 0.2 mm horizontally and 2 mm vertically have been observed (good statistics and a well defined edge). This is referred to as the "motion resolution" of the hodoscope. In terms of fuel quantity, this translates to the displacement of ~0.4 g of fuel by more than 3.6 mm horizontally or 22.5 mm vertically, for a seven-pin bundle. If only a single pin is being tested, if there is good signal-to-background (little nearby material that can obscure neutrons from the test fuel or scatter reactor neutrons into the hodoscope), if the reactor power is not changing rapidly, and if the counting statistics are adequate, the limits to the observable fuel motion might be an order of magnitude smaller. For the 122-cm collimator, the various detection limits are expected to be about twice as large as for the 51-cm instrument.

DYNAMIC RANGE

The fast-neutron detectors used to date have been "Hornyak button" scintillators.[1] It has been found feasible to use these detectors at counting rates approaching 10^6/s, although at such rates the corrections for deadtime and supralinear response become large. Data-collection intervals range from 1.5 ms to 12 ms or more, depending on the experiment. At the time the system was developed, the most satisfactory way to record the large quantities of data (336 channels each with up to 2^{12} counts per collection interval, leading to data-collection rates of $\sim 3 \times 10^6$ bits/s) was to display the scaler contents in binary form on a bank of neon lamps and photograph the array on high-speed film as the transient proceeded. The photographic method, however, has presented problems with variable image quality (stemming from a number of causes), and a system based on high-speed, multihead, magnetic-disk recording is being developed.

The Hornyak detectors have virtually no background rate that is independent of reactor power, because of their very low gamma sensitivity. Thus, the primary limitation in low-level counting is statistical--altough electrical noise from control-rod relays, etc., has sometimes been troublesome at very low counting rates. For some transients, meaningful hodoscope data have been accumulated for several seconds following reactor shutdown, albeit at considerably degraded time resolution.

DENSITY RESOLUTION

The ability to observe changes in the amount of fuel viewed by a channel depends on counting rate, signal-to-background ratio, required time resolution, and spatial extent of the change--that is, a one-channel change of borderline statistical reliability will be viewed with more credence if neighboring channels exhibit a correlated change. In the transient-overpower test E8, for example, fuel-quantity changes in 3 ms of the order

of 0.5 g/channel were significant if they occurred in a cluster of 4 or 5 channels or more. Near the time of peak power, an observed one-channel change of 0.36 g had a 50% chance of being merely a statistical fluctuation.

In tests to date, the background counting rate (in channels that were not viewing fuel) has typically been 1/4 to 1/2 of the rate in channels that viewed the center of a 7-pin bundle.

DEAD TIME AND SUPRALINEARITY

For reasons not fully understood, but probably related to the pileup of many low-amplitude gamma-ray pulses, the counting rate from the Hornyak detectors has been found to be supralinear with reactor power--that is, the counting rate tends to rise and fall more rapidly than the fission rate in the fuel under observation. It has been found that placing a few cm of lead in front of the detectors tends to reduce the problem somewhat, either by preferentially attenuating the gamma rays or by reducing the overall pulse rate. Some supralinearity remains, however (variable from channel to channel). A computer code has been developed to determine correction parameters, making use of the data that accumulate as the power rises but before fuel motion begins.

It has also been found that the effective dead time varies from channel to channel, so that for optimum results the dead times of many chanels need individual adjustment. Both the dead-time and supralinearity corrections can be derived concurrently from the same pre-motion data, and the procedure has given good results, at least in those transients where appreciable fuel motion did not occur much before peak power was reached (as in the TOP tests E7 and E8). The magnitude of the corrections needed is indicated by Fig. 3, which shows the average counting rate for the entire detector array as a function of time over the excursion portion of the E8 test. For individual scalers, some of the corrections would be greater than the averages shown, and some less. The effective dead times, for instance, ranged from less than 0.5 μs to greater than 5 μs.

ANALYSIS TECHNIQUES

One of the principal tools for interpreting the hodoscope data is the "differential hodograph," an example of which appears in Fig. 4. Such a representation shows, not the amount of fuel, but the change in the amount of fuel that occurred during a certain time interval. In the case of Fig. 4, the changes occurred between 26.6 s and the reference time of 7.5 s. A solid circle indicates an increase in the amount of fuel (i.e. in the power-normalized counting rate) in a hodoscope channel, and an open circle a decrease. The larger the symbol, the greater the change: the smallest ones represent a change of ∿0.5 g, and the largest ∿5 g. Conversion from power-normalized counting rate R/P to grams comes simply from subtracting the background R/P (average in channels that do not observe test fuel) from the average (corrected) R/P in the central channels. When combined with the knowledge that a central channel views ∿8 g of fuel (7-pin bundle), the result is a factor that converts change in R/P to grams.

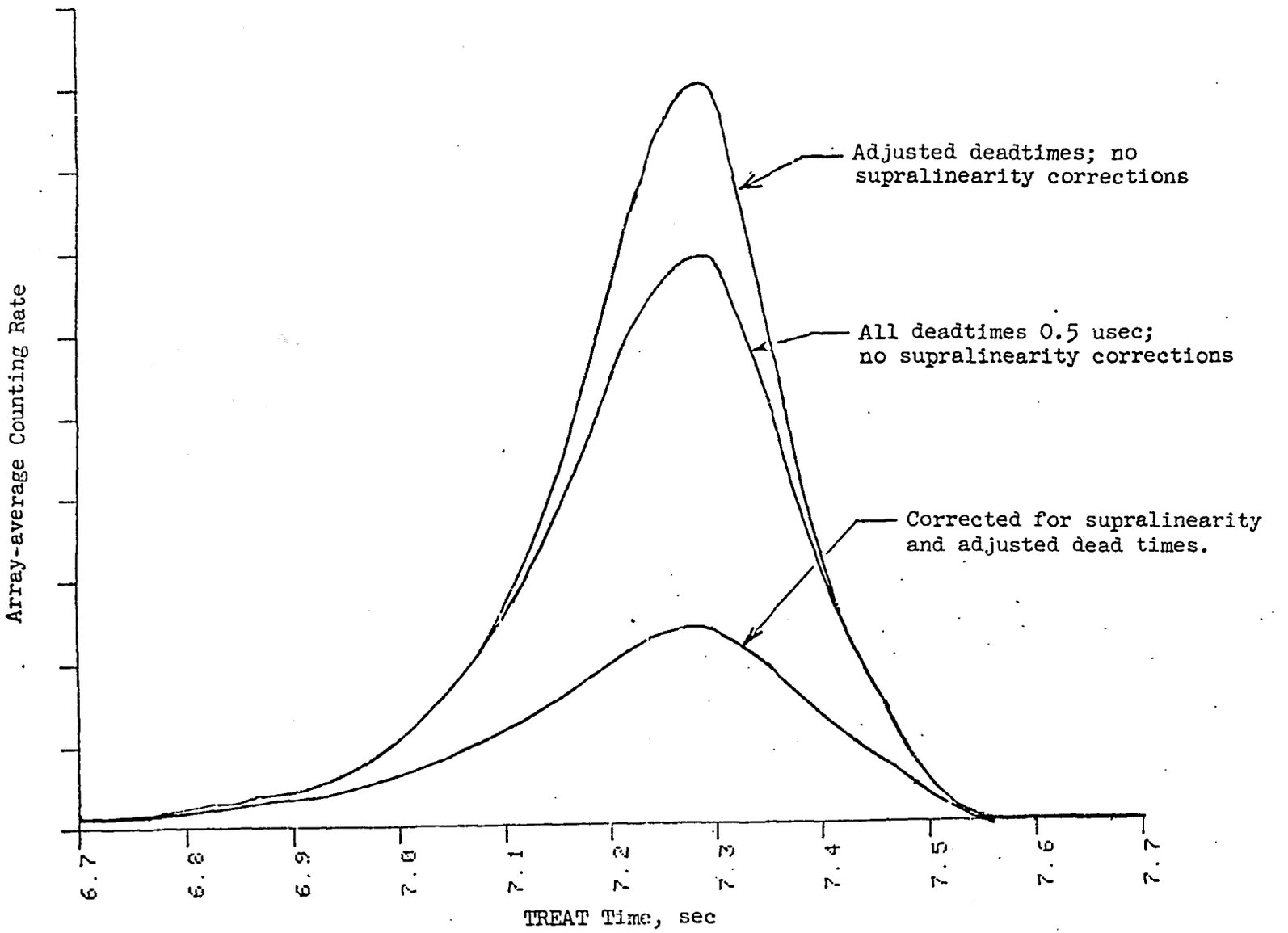

Fig. 2. Effect of Deadtime and Supralinearity on the Array-average Counting rate. Curves are normalized to equal amplitude at the preheat plateau. Transient E8.

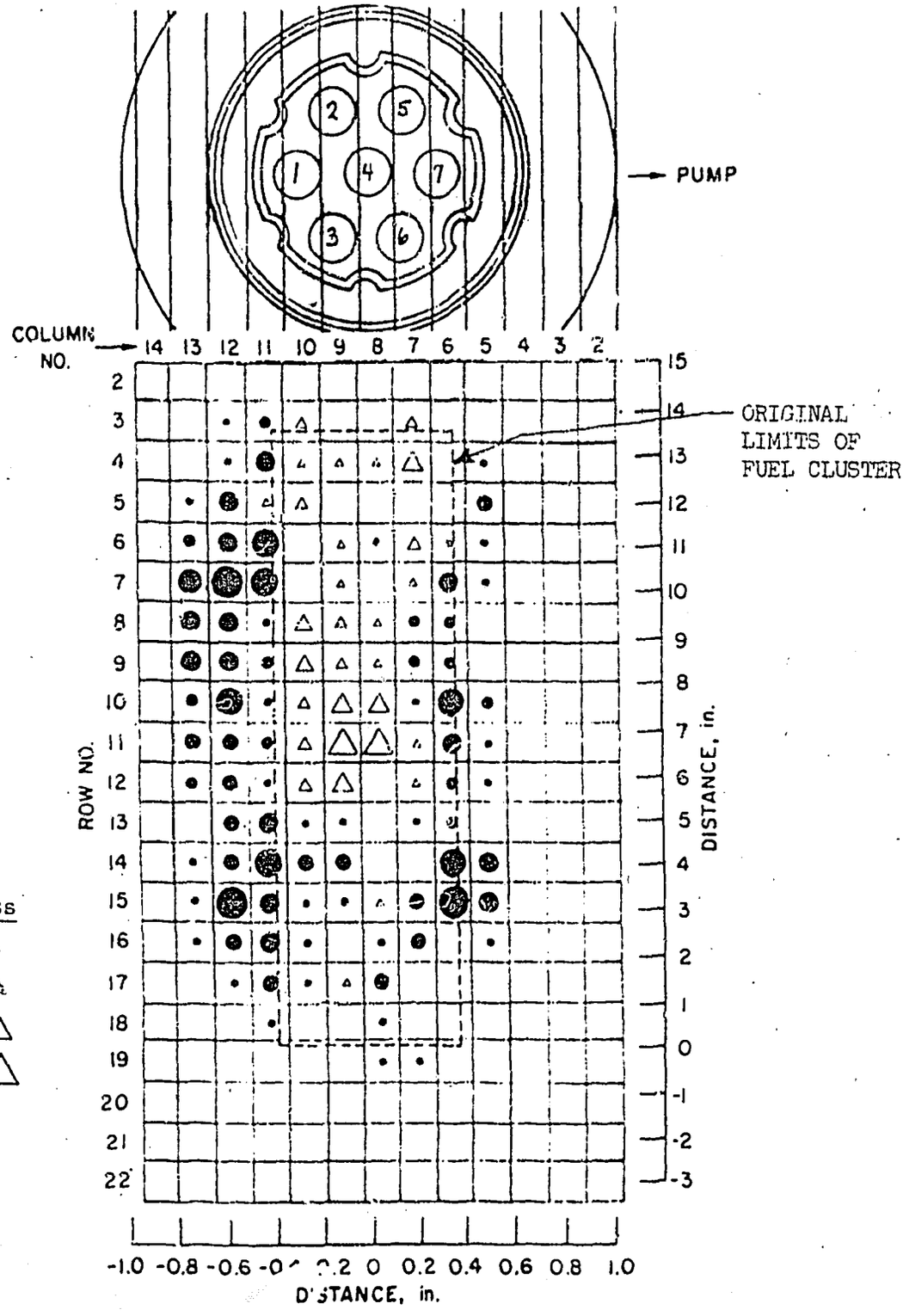

Fig. 4. Differential Hodograph, 7.5 - 26.6 s, Transient L4. The major slumping has just occurred, and the eructation is about to take place. The fluted tube has been thoroughly breached on the side away from the pump, and much of the fuel has left the midregion of the original fuel cluster.

Examples drawn from several of the TREAT power-transient experiments will now be given, to illustrate some of the methods used in analyzing the hodoscope data, and the type of results obtained.

TRANSIENT L4[3]

Test L4 was a loff-of-flow (LOF) experiment in which a 7-pin fuel bundle was preheated at 60 MW for 2 s, and then irradiated at a steady power of 34 MW (0.39 MW/m) as the sodium flow rate was cut off. After the coolant flow had ceased, the fuel melted, slumped, and then underwent an "eructation" in which some molten fuel was rapidly dispersed by vaporizing stainless steel. Figure 4 is a differential hodograph that shows the situation in the test chamber shortly before the eructation, Fig. 5, the configuration after the eructation, and Fig. 6, the net change that occurred during the eructation. (Figure 6 is, in effect, the difference between Figs. 4 and 5). It could be inferred from Fig. 6 that vapor generation at two different levels in the test chamber perhaps occurred coherently, leading to rapid compaction of molten fuel near the midplane. Examination of the event with greater time resolution, however, reveals that this was not the case -- that rapid fuel expulsion from the lower region occurred first, with, in fact, some doubt that the upper deficit was caused by vaporizing steel at all. The change that took place during the initial 20 ms of the eructation is shown in Fig. 7. Steel vaporizing below the midplane was forcing molten fuel upward.

The ability of the hodoscope to accumulate data following reactor shutdown is illustrated by Fig. 8, which shows a post-scram change that occurred in L4. Scram was at 30.2 s. To produce the differential hodograph of Fig. 8, the hodoscope data were averaged for the two half-second intervals 30.6-31.1 s and 31.6-32.1 s. The result supports pressure- and flow-sensor indications that a sudden event occurred at 31.3 s, by showing that a new upward fuel motion did occur at about that time.

TRANSIENT E7[4]

Test E7 was a transient-overpower (TOP) experiment, in which a 7-pin bundle was preheated for 2 s at 150 MW, and then subjected to a 3$/s ramp to a peak power of 2450 MW. The FWHM of the power peak was about 280 ms. Fuel motion began a little before peak power, and by the end of the test there had been considerable melting and repositioning of fuel, although there were no sudden relocations of large quantities of fuel. The most rapid fuel motion occurred at 7.72 s, with the power half-way down from the peak. The change that occurred in the 140-ms interval bracketing this motion are shown in Fig. 9. Prominent features in this picture are the accumulation of fuel on the pump side at Rows 7-12; th eloss of fuel from the upper left and lower portions of the original fuel zone; and the small increases in fuel content extending 100 mm or more below the bottom of the original test fuel region.

TRANSIENT H5[5]

The fuel motions in TOP test H5 were small. The ramp rate was 50¢/s, and the excursion was abruptly ended at a power of 600 MW, at which time pin failure was just beginning. Figure 10 shows the intermediate state of the motion. In the post-test examination of the pin remains, it was found

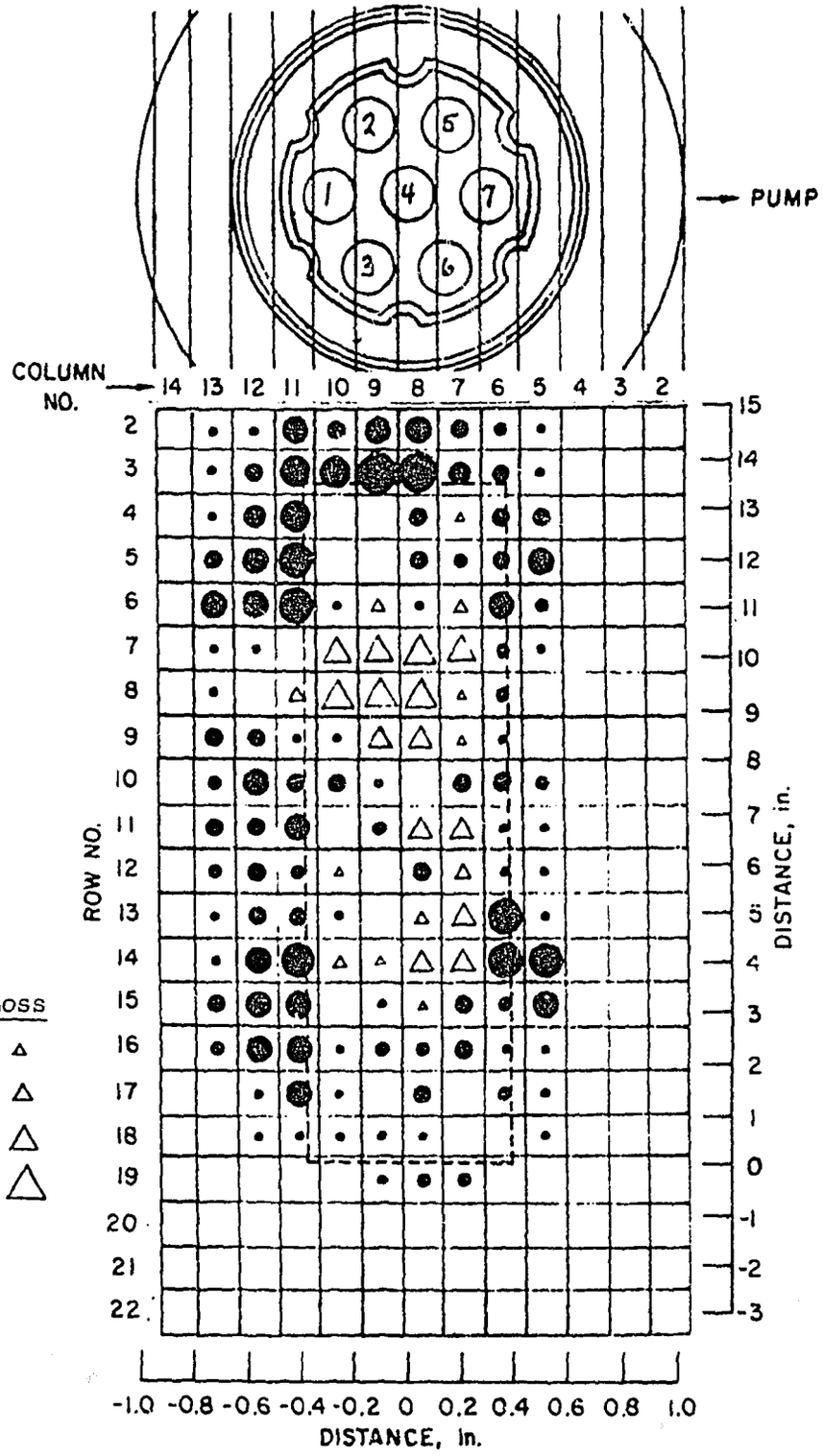

Fig. 5. Differential Hodograph, 7.5 - 28.1 Sec, Transient L4, Showing the Fuel Distribution Following the Eructation.

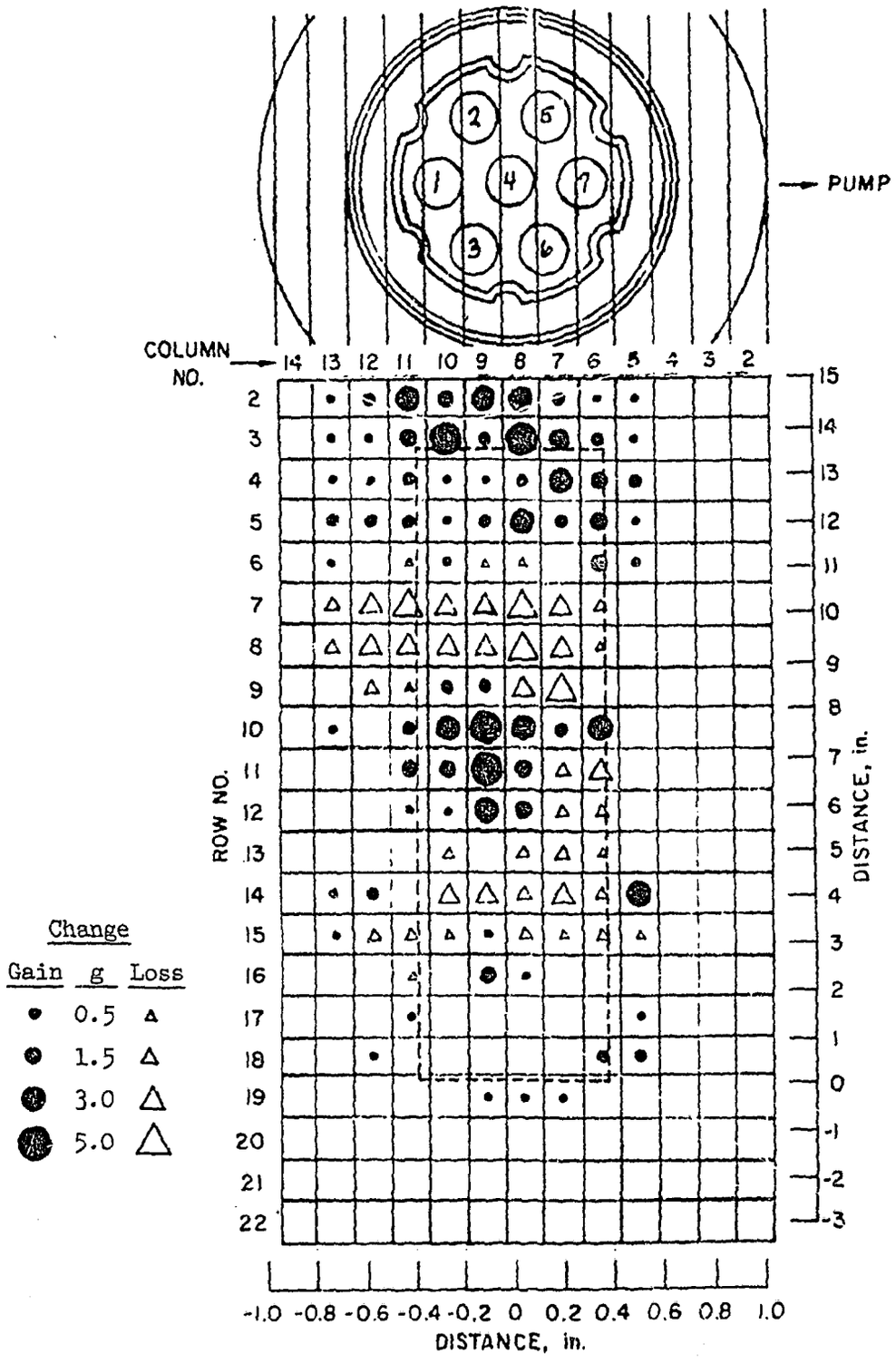

Fig. 6. Differential Hodograph, 26.6 - 28.1 Sec, Transient L4, Showing the Change in Fuel Configuration Brought About by the Eructation. Very little fuel moved downward. The regions of deficit correlate with previous regions of surplus.

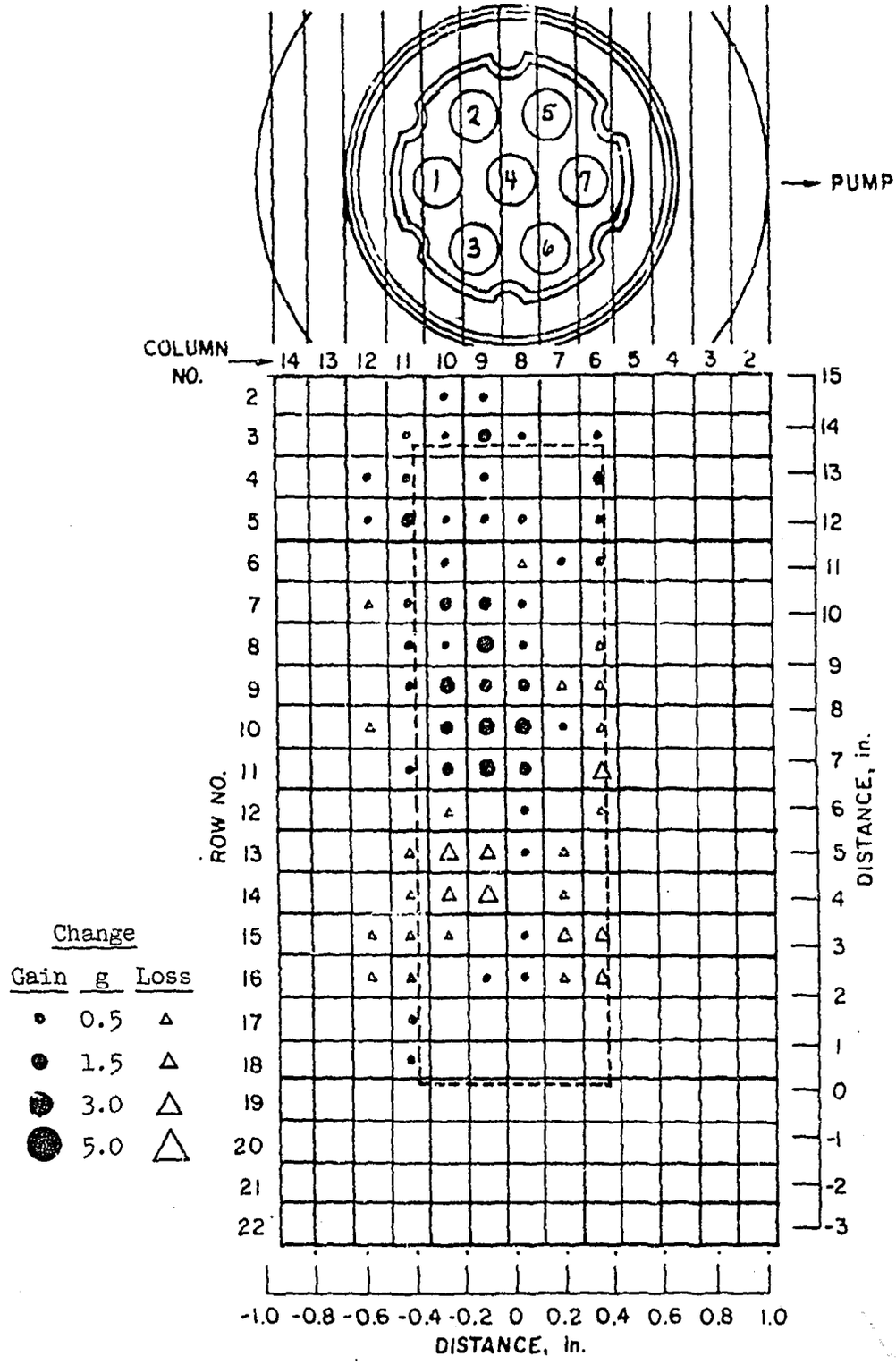

Fig. 7. Eructation Detail, 26.925 - 26.945 Sec. (Start of eructation.) Test L4.

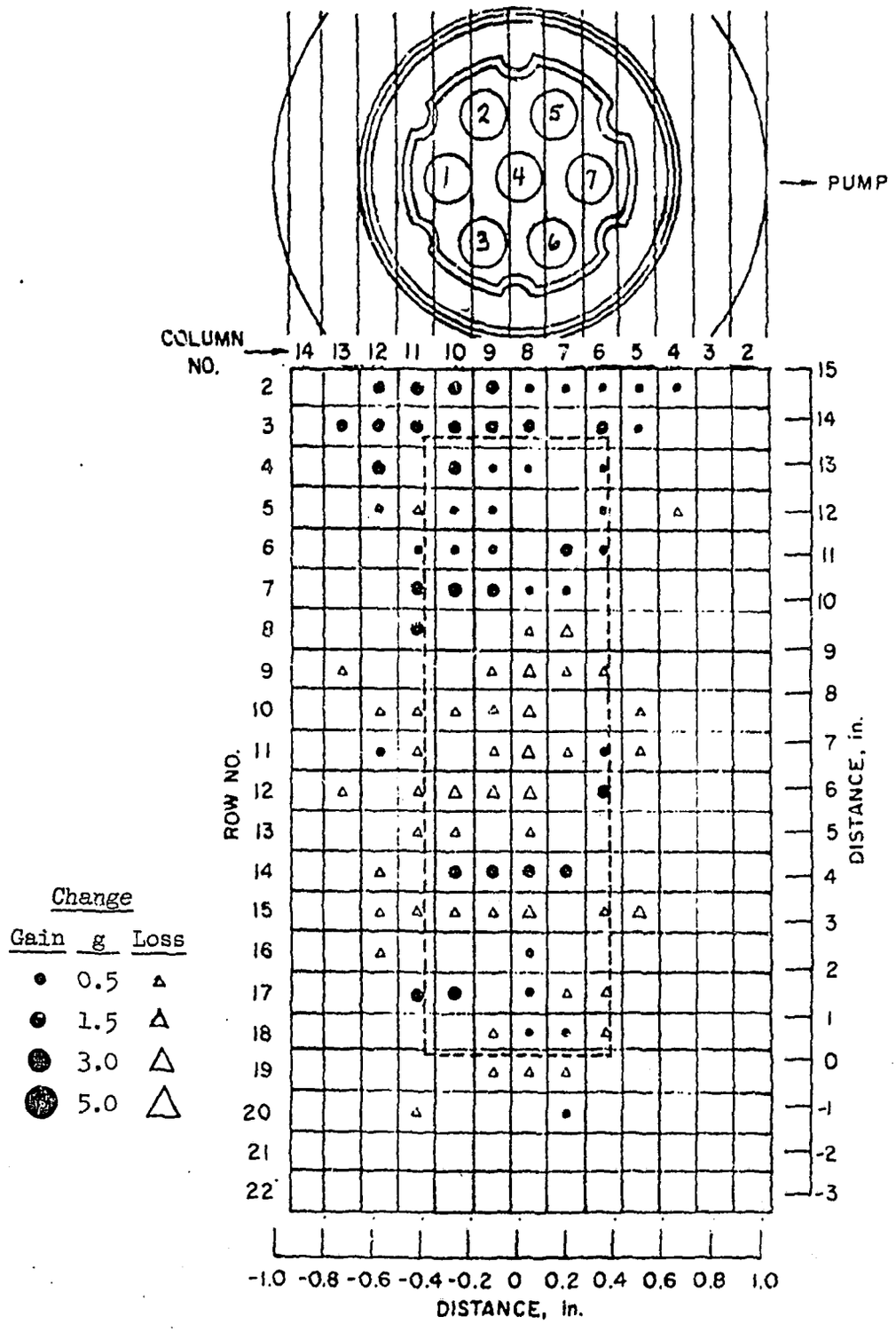

Fig. 8. Differential Hodograph, 31 - 32 s (Post-scram), Transient L4.

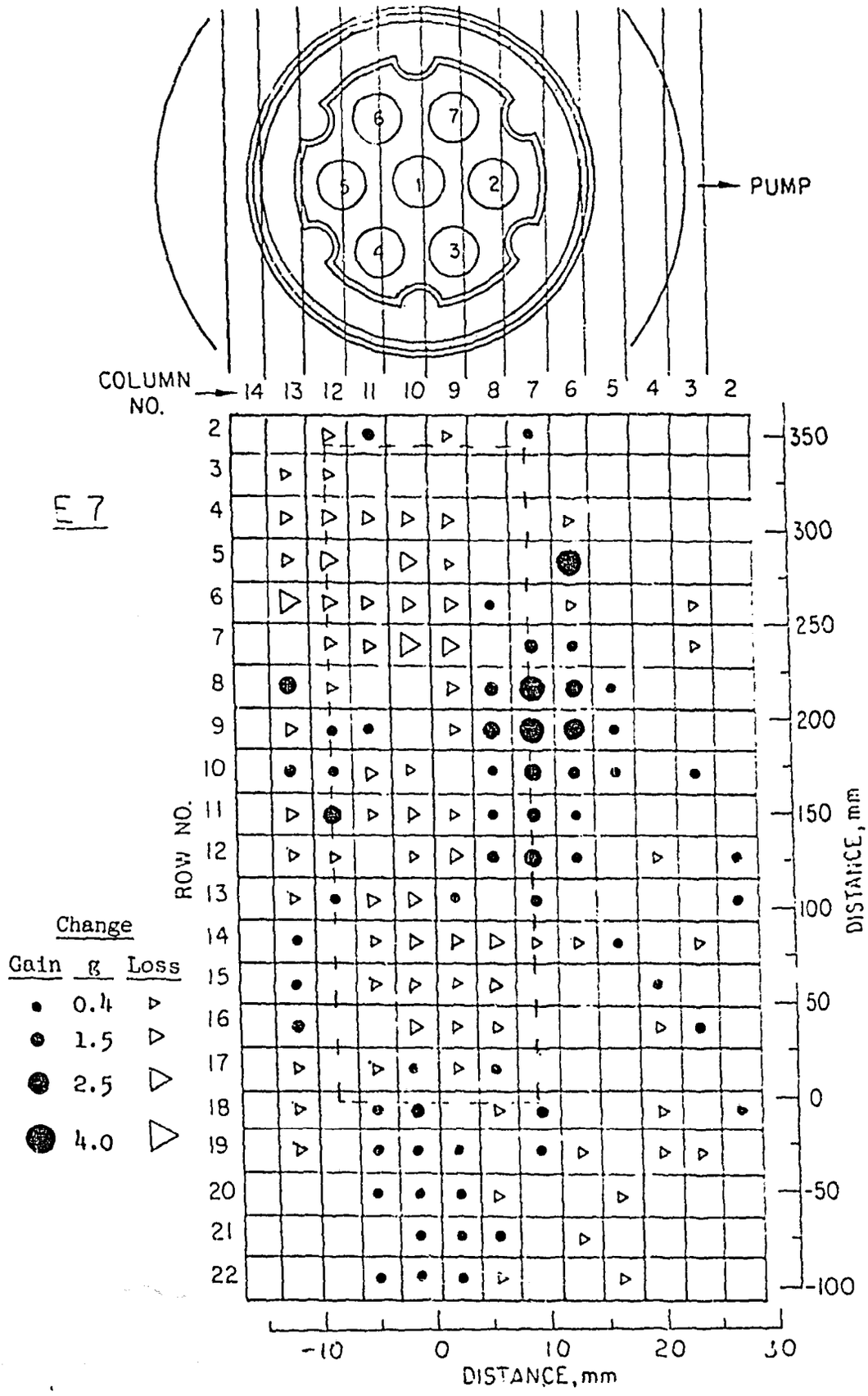

Fig. 9. Short-term (140 ms: 7.63 - 7.77 s) Differential Hodograph from E7, Showing Penetration of the Fluted Tube at the Pump Side, Small Amounts of Fuel below the Original Fuel Zone, and Considerable Loss of Fuel from the Original Fuel Zone.

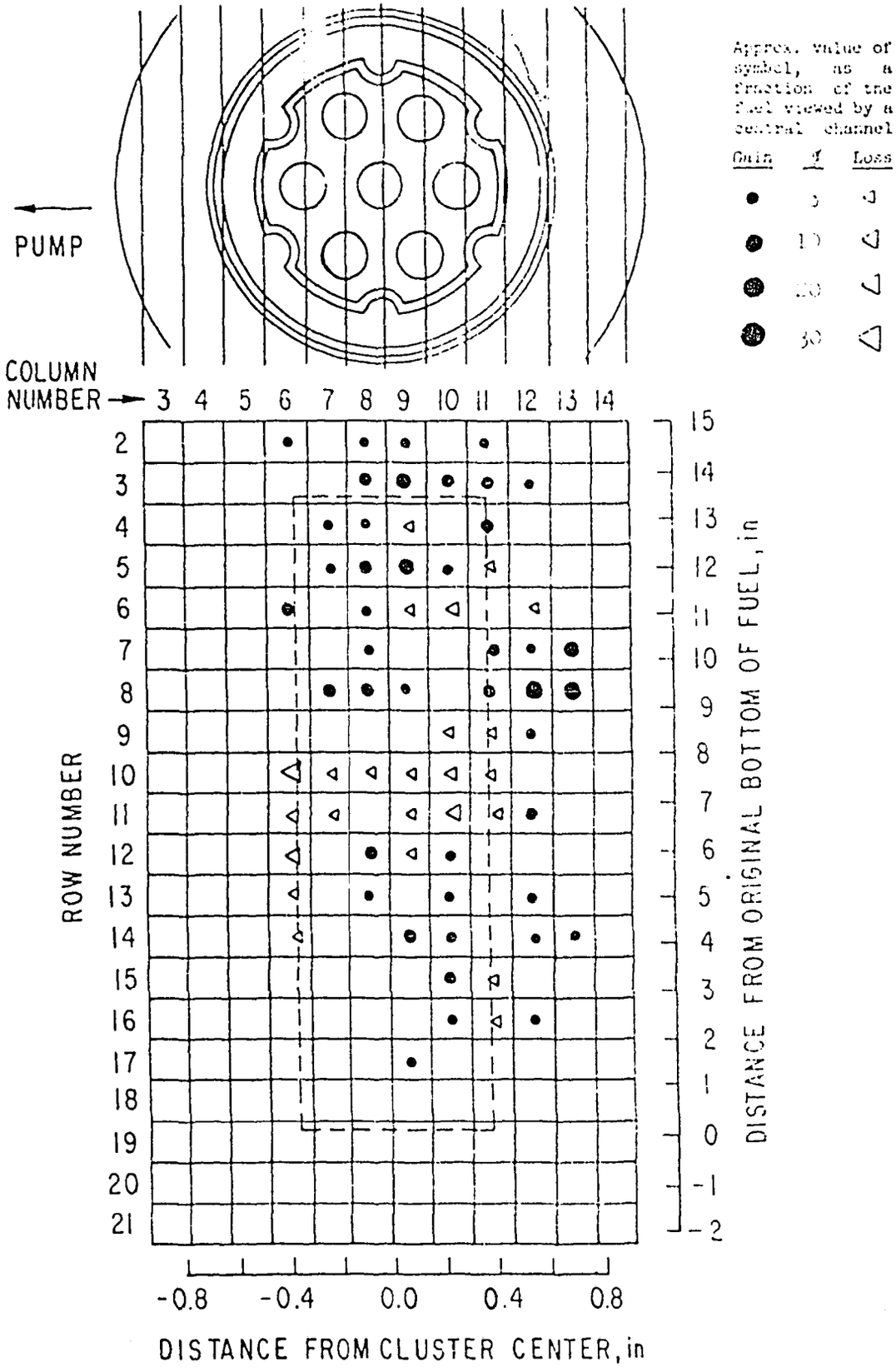

Fig. 10. Short-term (70 ms: 8.08 - 8.15 s) Differential Hodograph from H5, Showing Small Penetration of Fluted Tube on Side Away from Pump, Minor Levitation of Upper Portion of Fuel, Small Amounts of Fuel Moving Upward and Downward from Midplane, and Minor Loss of Fuel near Midplane.

that little fuel had been lost from the central (irradiated) pin. However, there were central "gun barrel" voids in five of the six (fresh) peripheral pins, the result of central melting with downward flow and some expulsion. Particles of fresh fuel were found above the fuel zone, between the pins. The fuel motion depicted in Fig. 10 is deduced to be a combination of: (a) pin bowing; (b) cluster deformation, leading to a net horizontal movement away from the pump; (c) expulsion of solid oxide particles from the irradiated pin and molten fuel from the fresh pins; (d) upward movement of some of the expelled material; (e) flow of molten fuel within the hotter pins; and (f) possibly some levitation within cladding of the upper half of some of the fuel columns by expanding gas.

TRANSIENT HUT5-3A[6]

An alternative and sometimes useful way to present the hodoscope data is in the form of graphs of detector response vs time. To emphasize the fuel-motion effects rather than power changes, the quantity plotted is usually the power-normalized counting rate R/P, where R is the observed counting rate in a scaler or group of scalers (corrected for dead time and supralinearity), and P is proportional to the reactor power. In analyzing HEDL shot HUT5-3A, the data were analyzed on the basis of row-averaged and column-averaged R/P curves.

HUT5-3A was a single-pin test with a 50¢/s reactivity ramp that was terminated by scram shortly after fuel motion began. The fuel pin was surrounded by NaK, nickel, stainless steel, and graphite to a total thickness of ∿75 mm (see Fig. 11). The hodoscope total signal-to-background ratio was ∿2, as shown in Fig. 12. Of particular interest was the vertical component of the fuel motion. Figure 13 shows the vertical motion in the top five rows of channels during a selected 350-ms interval encompassing the principal fuel motion. Changes of ∿200 mg in the amount of fuel in a row can be discerned above the statistics. In this test, the 343-mm fuel column extended from Row 3 to Row 18 in the hodoscope field. The error bars indicate an 85% confidence level. By 12.7 s, the power is low and the statistics have become poor.

TRANSIENT E8[7]

TREAT test E8 was a TOP experiment with seven pins, in which a 2.2-s preheat plateau preceded a power burst to 2525 MW. Considerable fuel relocation occurred. The excursion portion of the power curve is shown in Fig. 3. Differential hodographs covering the time of initial fuel motion are given in Fig. 14. Interpretation of these diagrams is as for the ones of Fig.4 et seq., the difference in appearance stemming from the fact that Fig. 14 was generated by computer. Small amounts (order of a few grams) of fuel can be seen to have left the right side of the original fuel cluster, to appear in a thin dispersion above the fuel region.

Figure 15 shows the changes in axial distribution of the test fuel over the course of the transient.

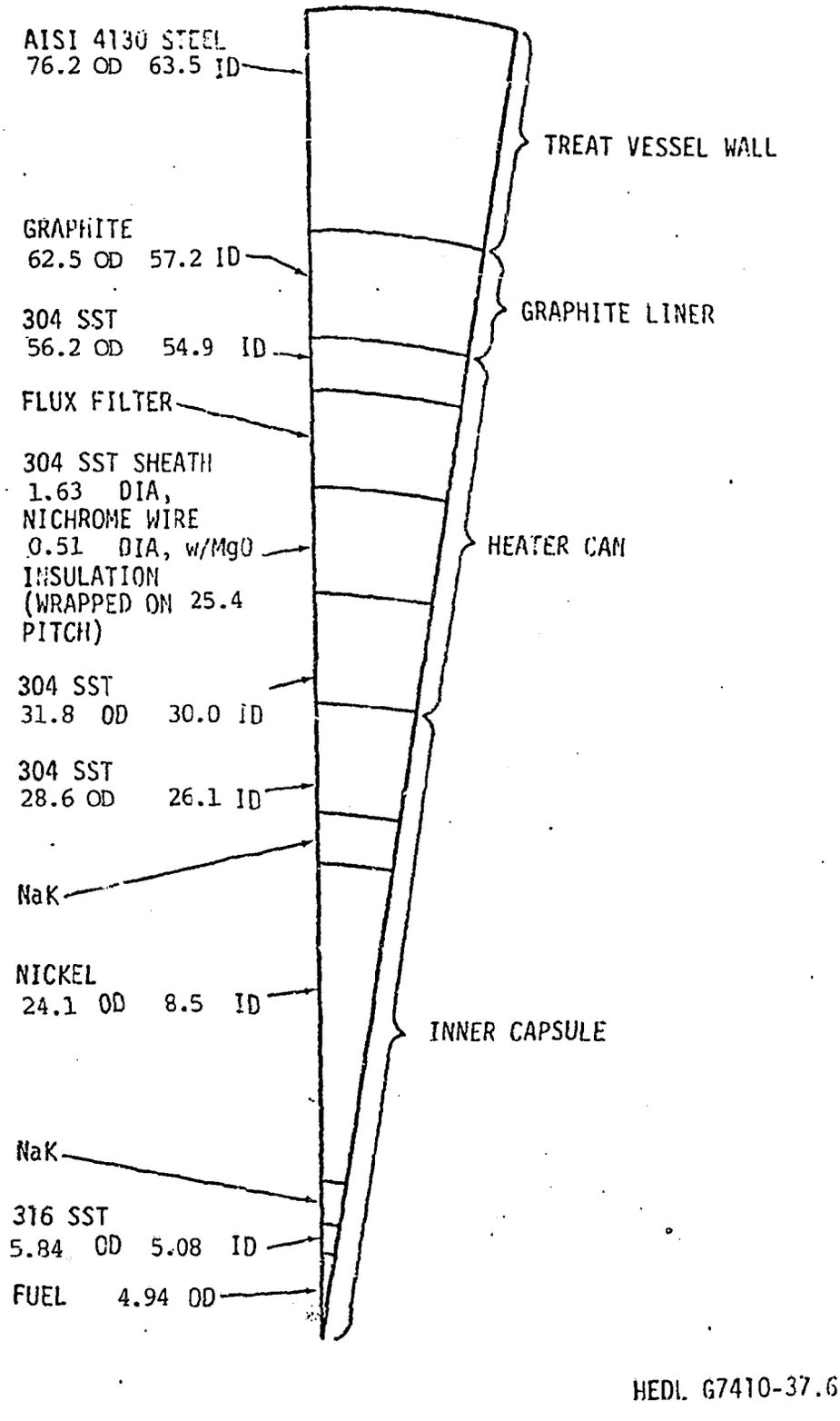

Fig. 11. Radial cross-section of HEDL capsule at TREAT core midplane. Dimensions in millimeters.

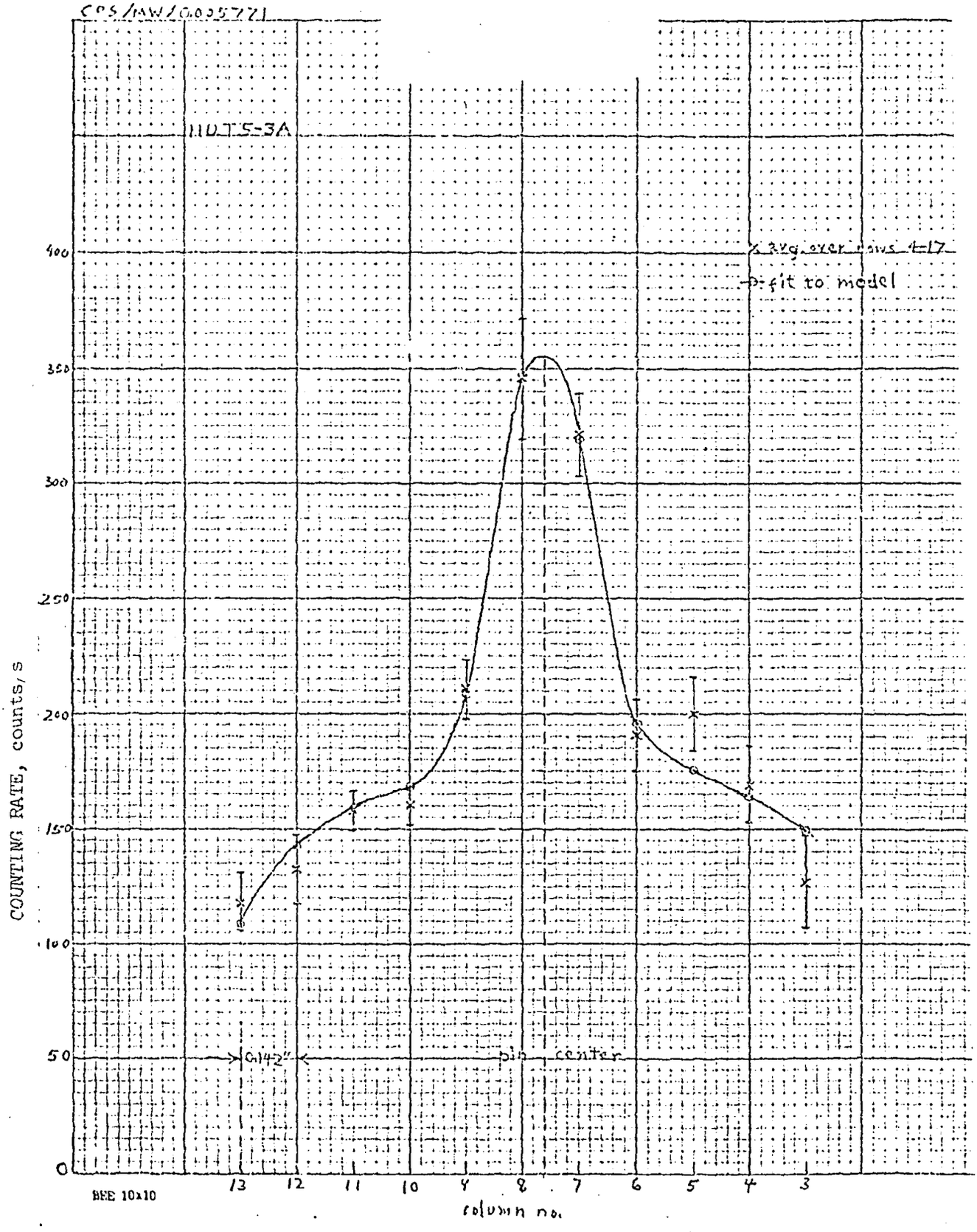

Fig. 12. Radial Profile of Test Fuel, HUT5-3A. Data averaged over Rows 4 - 17.

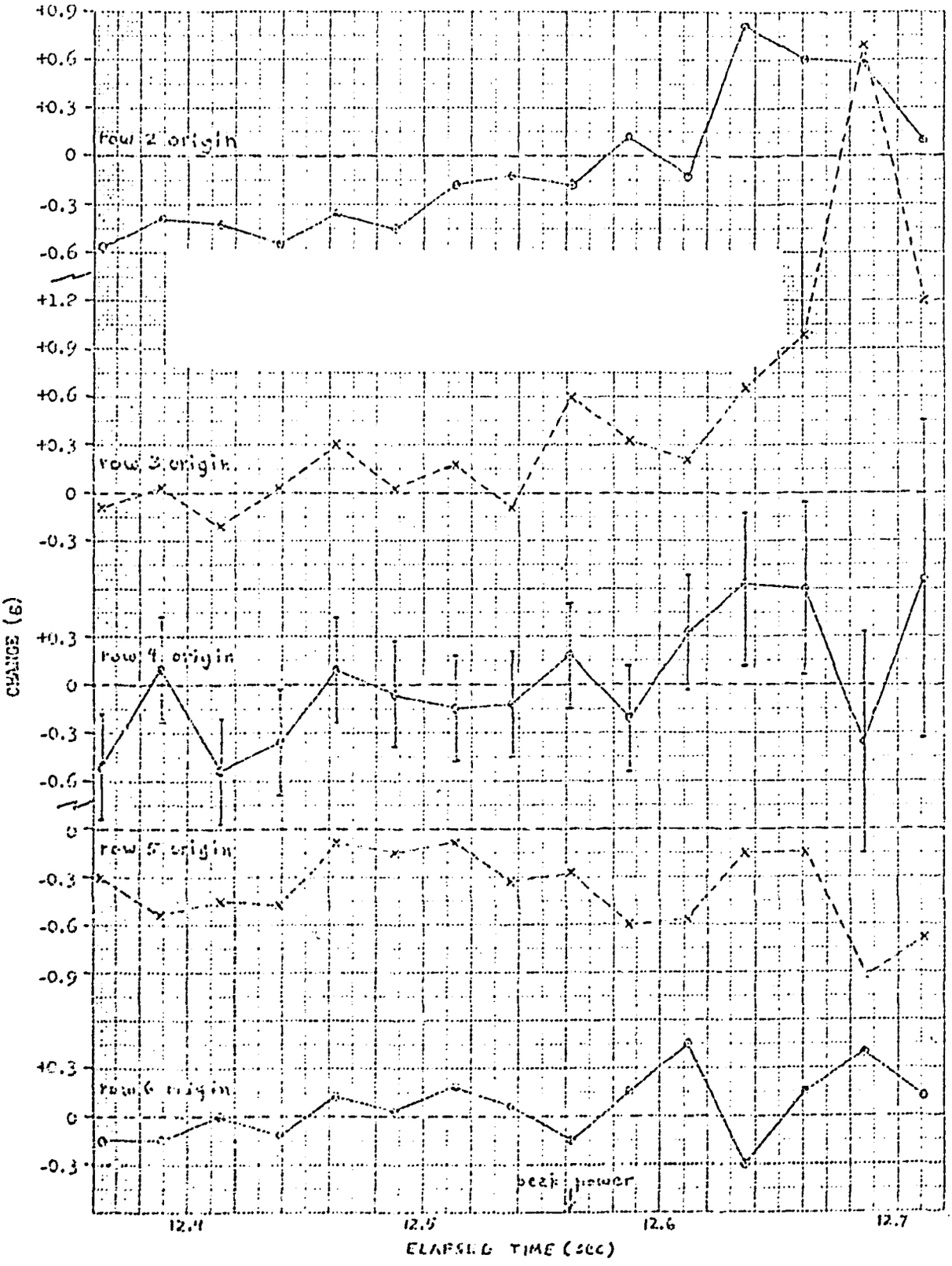

Fig. 13. Fuel-Quantity Changes for Rows 2 - 6, with Respect to Pre-motion levels. Summed over Cols. 6 - 9. Test HUT5-3A.

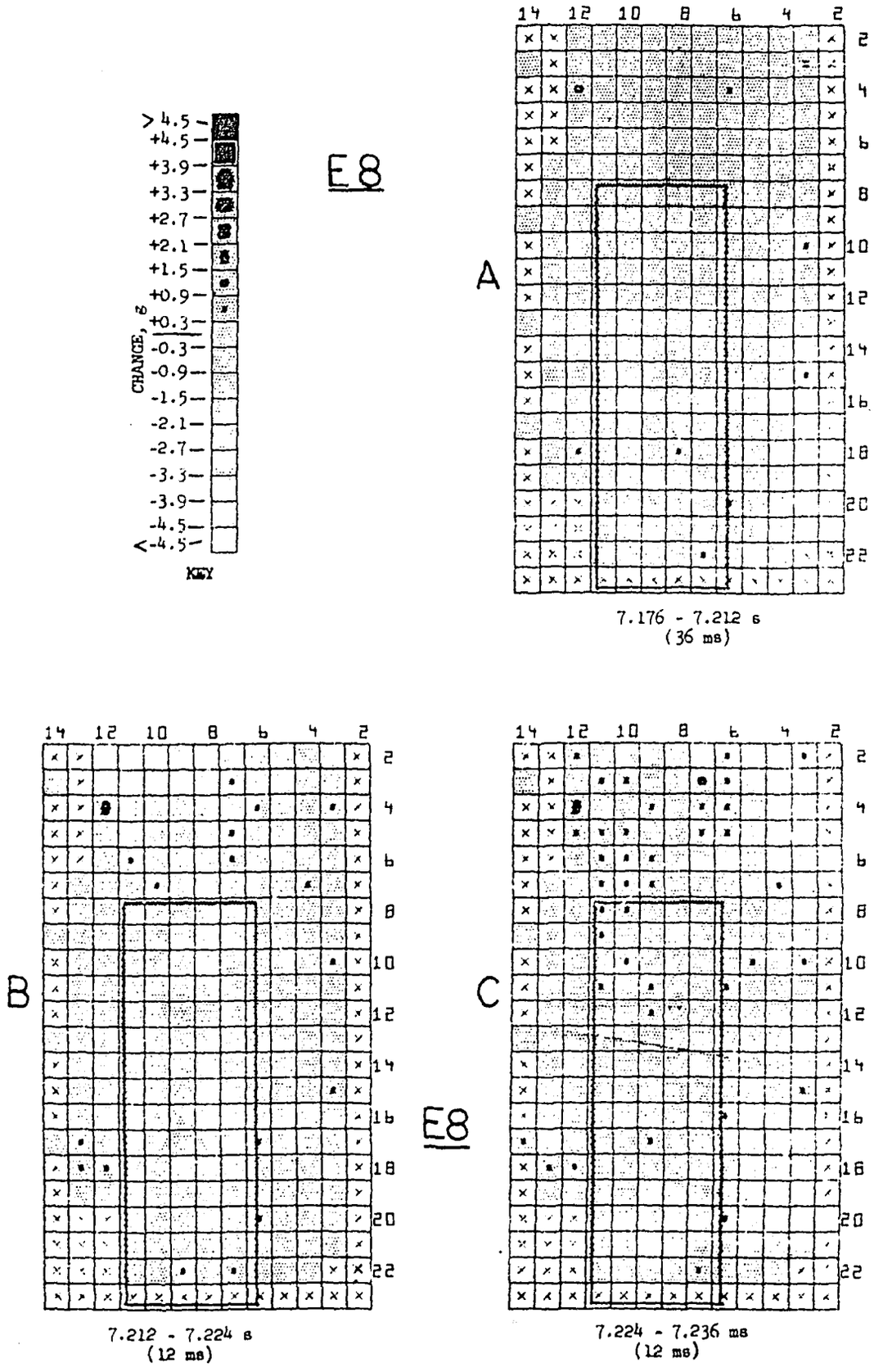

Fig. 14. Differential Hodograms for E8: 7.176 - 7.236 s. Referenced to prefuel plateau (4.53 - 6.65 s). Scale maximum: 4.5 g fuel. The data-averaging interval is given below each hodograph.

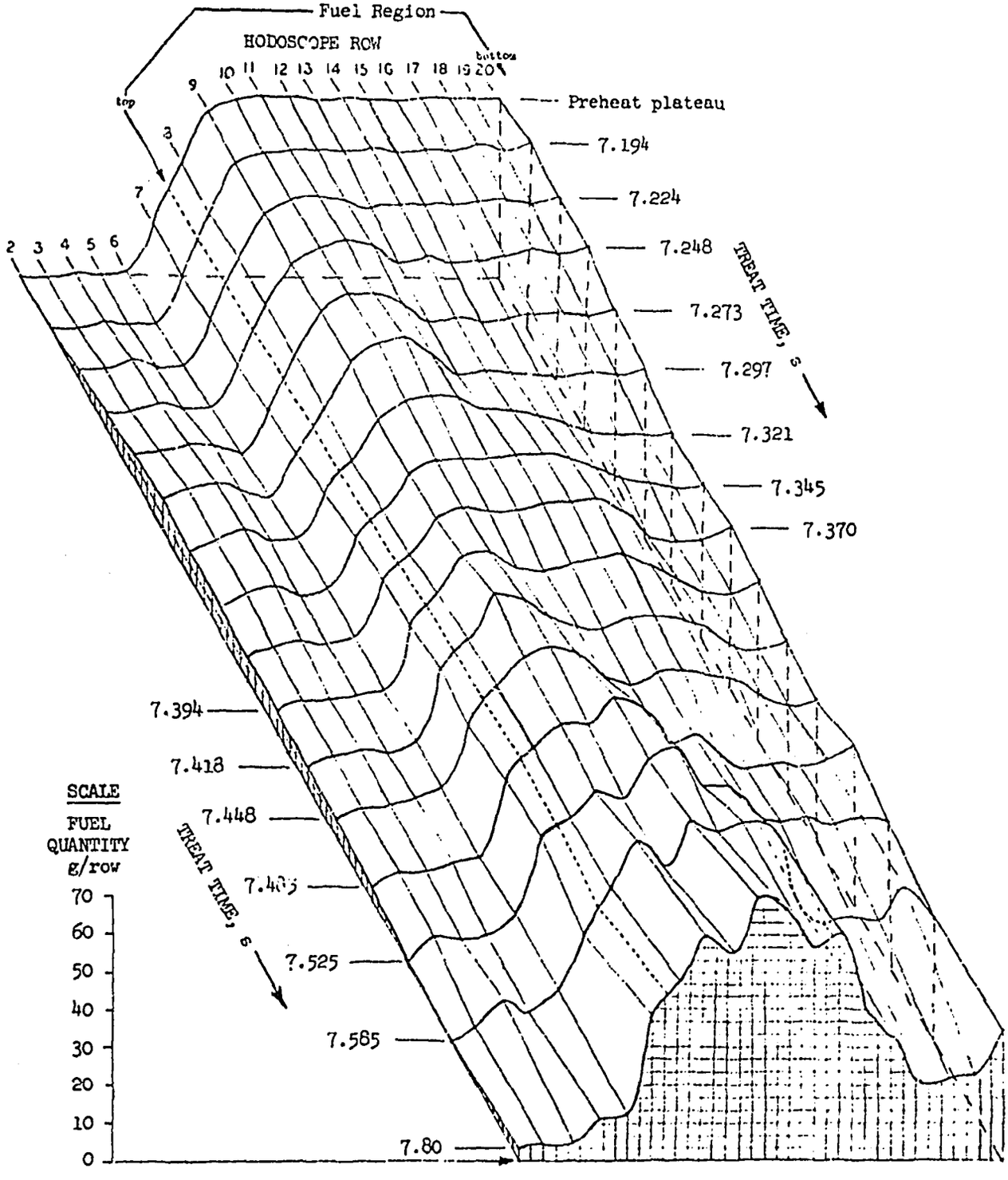

Fig. 15. Axial Fuel-Quantity Profiles in Transient E8. The data for each row are averages over Cols. 5 - 13. Time runs from top to bottom. The times given are the midpoints of the averaging intervals, which are not all of the same duration. To convert the mass scale to grams per mm of axial height, divide by 22.5 mm/row.

TRANSIENT L5[8]

In test L5, a rapid power excursion was initiated when the cladding had reached its melting point, after sodium flow was shut off. The 51-cm collimator observed a bundle of three 854-mm fuel pins, which extended both above and below the viewing area. During the transient several changes in the total amount of fuel viewed were recorded as the pins expanded, buckled, and underwent local voiding. Those changes can be seen in Fig. 16.

The interpretation of the fuel changes in the various time spans indicated in Fig. 16 is given in Table 2. Those deductions are based, not only on the overall fuel-mass changes, but also on a more detailed look at the hodoscope data and loop-instrument readings as correlated with calculational predictions.

TABLE 2. SCENARIO FOR TEST L5

Time Spans No.	Time, s			Fuel Motion
I	3.0	-	10.0	Stable, no fuel movement.
II	11.0	-	11.9	Apparent influx of fuel.
III	11.9	-	12.5	Abrupt outflux of fuel due to localized voiding, then a balance of fuel outflux to influx.
IV	12.5	-	13.0	Further localized voiding followed by a gradual net influx of fuel.
V	13.0	-	13.5	Localized voiding slows, effecting a net balance of fuel influx to outflux.
VI	13.5	-	13.7	Localized voiding halts with increased fuel mass collected above and near the midplane of the fuel column.
VII	13.7	-	13.8	Axial voiding of fuel column; the major fuel motion is dispersive and upward.
VIII	13.8	-	14.4	Large accumulation of fuel in the upper region above the initial fuel midplane.

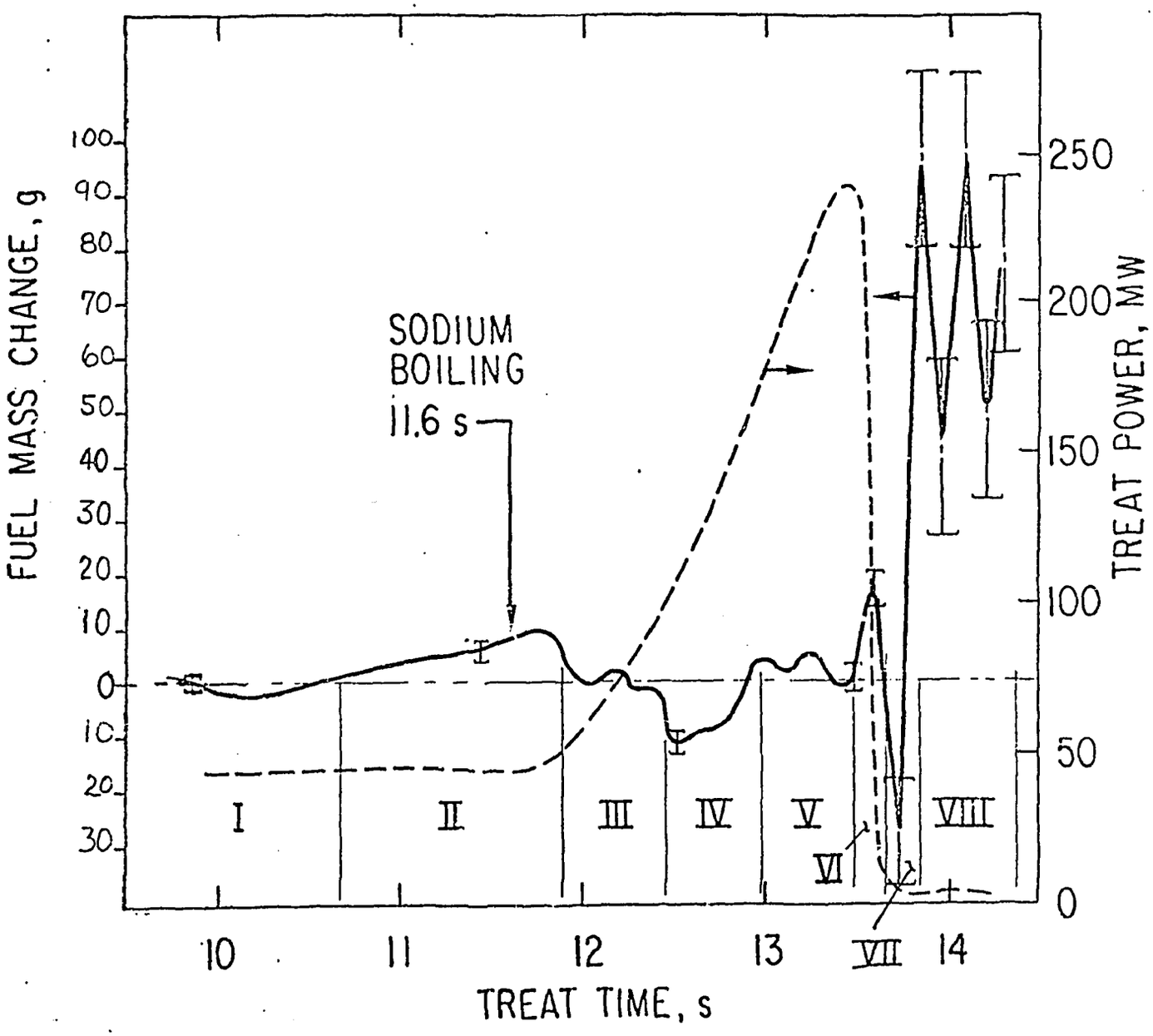

Fig. 17. Change in the Total Mass of Fuel Viewed by the Hodoscope, as a Function of TREAT Time. Test L5.

SUMMARY

A fast-neutron hodoscope has been operational at the TREAT reactor since 1965. In 1969, the number of detector channels was expanded from 50 to 334, with a field of view capable of including a bundle of 343-mm fuel pins. Recently a new collimator has been installed to encompass full-length 914-mm fuel. Since there has been only limited experience with the new collimator to date, the discussion concerns primarily the original, "51-cm" collimator.

Under good conditions, the hodoscope has been able to resolve fuel-boundary motions of as little as 0.2 mm horizontally and 2 mm vertically; with a seven-pin fuel bundle, displacements of 400 mg of fuel (70% enriched) can be detected. With a single fuel pin, a change of as little as 50 mg, under the best conditions, can be statistically significant. For fast transients, data-collection intervals as short as 1.5 ms can be used. At the low-counting-rate end of the scale, meaningful hodoscope data have been accumulated, with degraded time resolution, for several seconds following reactor shutdown.

At the higher counting rates, many channels require individual dead-time corrections, and most must be individually adjusted for supralinearity--the tendency for the counting rate to increase more rapidly than the fission rate in the observed fuel. At high reactor powers, the counting-rate corrections can be large, leading to a reduction in the observed rate by 75% or more, depending on the channel. Counting rates up to 10^6/s have yielded useful results.

Examples drawn from various TREAT tests illustrate identification of fuel-motion phenomena such as: gross slumping (L4); lateral motion through the flow-tube wall (L4 and E7); the beginning of a rapid fuel dispersal ("eructation") driven by vaporizing stainless steel, and the net relocation due to that event (L4); transport of gram-quantities of fuel below the fuel zone (E7) and above it (H5 and E8); initial loss of small amounts of fuel from near the midplane (E8); changes in total amount of viewed fuel as the pins expanded, buckled, and underwent local voiding (L5); small vertical motions in a single-pin test (HUT5-3A); and changes in axial fuel distribution in a TOP test involving extensive fuel relocation (E8).

ADDENDUM 1.

NORMALIZATION OF HODOSCOPE DATA AND CONSERVATION OF FUEL MASS

Examination of the differential hodographs for L4 reveals an apparent gain in the total amount of test fuel as the transient proceeded. Some of the possible reasons are discussed in Appendix I of Ref. 3, wherein the following candidate explanations were considered: (1) decreased scattering of high-energy neutrons as the sodium voided from the test region; (2) diminished self-shielding in the test fuel as it spread over a larger region; (3) supralinearity in the response of some of the hodoscope channels; (4) an increase in the efficiency of some of the channels as the transient progressed. The overall conclusion was that the first three possibilities were not able to account for the magnitude of the observed effect in L4, although each might have been making a small contribution.

In the case of Item 2, for instance, it has been calculated that a uniform dispersal of the test fuel over the test cavity could cause as much as a 20% increase in calibration factor (and hence in fission rate), if the fuel were highly enriched and there were no thermal-neutron filtering. However, this was ruled out as the cause of the L4 drift by the observation that a similar drift occurred in the calibration test, L4-1, wherein there was no fuel dispersal (nor sodium voiding). Further, there was no obvious time correlation between changes in array-average counting rate and fuel dispersal in L4-2. Thus we are left, by default, with the postulate that something was causing the efficiency of some (not all) of the channels to change with time as the reactor power was held approximately constant.

Two possible causes of such an effect come to mind: (a) an increase in intense, low-energy gamma background as the fission products accumulated in the test region, leading to increased ambient light level in the Hornyak scintillators, with consequent acceptance by the discriminators of lower-energy pulses; and (b) increase in photomultiplier gain or dark current, or both, under the high-pulse-rate conditions. The latter effect, in particular, is likely to be highly variable from channel to channel, and such variation was, in fact, present.

Complete resolution of this phenomenon, while interesting per se, is not central to the analysis of fuel motion in TREAT transients. The reason the problem is not central is that it disappears (in first approximation) if the counting rates in the hodoscope channels are appropriately normalized -- specifically, by building into the reference power curve a time drift that is proportional to the increase in overall (power-normalized) counting rate. If no more than small amounts of fuel are lost from the field of view of the hodoscope, the simplest way to do this is to relate the observed counting rate in each scaler to the average counting rate for the whole array. If a significant amount of fuel does leave the field of view, then a synthetic power curve can be constructed with sufficient accuracy (remembering that ±20% or so in an observed change is adequate).

The second-order effect that remains after such compensation is the channel-to-channel variability. Because of this variability, a change in observed counting rate in any one channel is viewed with low credence unless supported by correlated changes in adjacent channels.

The L4 test (Figs. 4 - 8) and the H5 test (Fig. 10) were analyzed before the ability to make supralinearity corrections and to normalize to the array average had been implemented. Since then, extensive work has been done to generate the corrections for supralinearity and dead time that are mentioned in the body of this report and described in more detail in Addendum 3. A rework of the L4 and H5 data now would lead to differential hodographs that would come considerably closer to conserving fuel mass, as they should.

An additional cause of apparent non-conservation, in any representation like a differential hodograph should be kept in mind: In constructing such a figure, it is necessary to establish a threshold below which a counting-rate change is considered to be zero for purposes of the diagram. This means, for instance, that if a small amount of fuel -- say 0.15 g -- were to leave each 30 channels and become concentrated elsewhere in a group of 10 channels, the resulting differential hodograph would show increases in those 10 channels, with no indication whatever of where the fuel came from. This applies, of course, to data from any fuel-motion sensor -- not only to hodoscope data.

There is still another factor pertaining to perceived degree of fuel conservation that applies not only to a neutron hodoscope, but to any other method that makes use of radiation emitted by the fissioning fuel -- namely, axial gradients in neutron flux, due to the natural buckling of the reactor flux and to any flux-shaping methods that might be used in setting up the test. The result of these gradients is that, as fuel moves into a region of lower flux (e.g., as it moves upward into the shadow of a boron flux-shaping collar), some of it will tend to *disappear*, as far as the detecting instrument is concerned. In analyzing hodoscope data, it has been our practice to increase the channel-efficiency corrections as a function of distance from the midplane, by requiring that the background rate be independent of axial position. It is recognized, however, that this does not necessarily lead to proper compensation for the effects of flux-shaping collars, *although it should compensate for* reactor buckling. The best we can say is that there have been no obvious problems, and that agreement between hodoscope observations and post-mortem examinations for such regions has generally been good.

The various normalizations and supralinearity compensations have been quite adequate to date for analysis of TREAT experiments. We anticipate, however, that more sophisticated models will eventually be developed, to assist in refining the connection between experimental data and fuel-density changes.

ADDENDUM 2.

ON THE DETECTION OF SMALL MASS CHANGES

In the sections on spatial and density resolution in the body of this report, it is mentioned that counting-rate changes corresponding to mass changes of about 0.4 g (with a 7-pin fuel cluster) tend to be statistically significant. To avoid confusion, we would like to emphasize that this definitely does not mean that large mass changes can be measured with a precision of ±0.4 g. What perhaps should have been said is that mass changes, in the case of a 7-pin fuel bundle, can typically be measured with a precision of ±20% or ±0.4 g per channel, whichever is greater.

For example, three pins in a line contain approximately 8 g of fuel within the viewing area of a single hodoscope channel. Loss of 0.4 g from such a channel (5% loss) would typically result in a statistically significant change in counting rate, with perhaps a 50% confidence level. Note that here the probable error in the observed change is greater than 20% -- amounting, in fact, to ±100%. On the other hand, loss of a total of 20 g of fuel from a cluster of five channels would be measured with a precision of about 20% (±4 g).

For further clarification, see the "rule of thumb" expressed in the "Ex-Vehicle Instrumentation" section of Ref. 9.

ADDENDUM 3.

DEADTIME AND SUPRALINEARITY CORRECTIONS

The Hornyak-button detecting channels of the hodoscope exhibit a nonlinear response to changes in reactor power, the extent of the nonlinearity being highly variable from channel to channel. Detailed examination of this nonlinearity has led to the conclusion that it is probably caused by pileup of small gamma and neutron pulses, and that the nonlinear increment is proportional to the square of the counting rate Co that would be observed in the absence of the nonlinearity. This model can be expressed by

$$Cm / (1 - Cm\ \theta) = Co + A\ Co^2,$$

where Cm is the measured counting rate before deadtime corrections, A is a constant that is a measure of the supralinearity of the detector response, and θ is an adjusted deadtime correction.

Under the assumption that Co is proportional to the reactor power, the optimum values of A and θ are determined with the aid of the computer code SUPRA. For a given value of θ, SUPRA determines A by a least-squares fitting procedure. The parameter θ is iterated to achieve an approximately flat plot of A as a function of reactor power P for high values of P (with the fit terminated prior to fuel motion). While θ appears as a deadtime in the formula, it does not necessarily physically represent a deadtime. Rather, it is used in conjunction with A to provide a two-parameter supralinearity correction: On occasion, negative values of θ are needed for best fit to the data. This is interpreted to mean that factors in addition to those leading to the quadratic dependence mentioned above may be important.

The values of A and θ found by this procedure are used in the final processing of the hodoscope data.

REFERENCES

1. A. De Volpi et al., "Fast-Neutron Hodoscope at TREAT: Development and Operation," Nuclear Technology 27, 449-487 (1975).

2. A. De Volpi, "Current Developments in TREAT Hodoscope Technology," Trans. Information Exchange Conference on Reactor Fuel and Clad Motion Diagnostics, Albuquerque, N. M., November 11-12, 1975.

3. G. S. Stanford, et al., "Final Analysis of Hodoscope Data for Transient L4-2," Internal ANL/RAS Memorandum, Dec. 18, 1975.

4. G. S. Stanford, et al., "E7 Fuel Motion from Hodoscope DATE: Final Report," Internal ANL/RAS Memorandum, May 20, 1976.

5. G. S. Stanford, et al., "Finald Analysis of Hodoscope Data for Transient H5," Internal ANL/RAS Memorandum, April 14, 1976.

6. E. A. Rhodes, et al., "Hodoscope Fuel Motion Analysis of TREAT In-Reactor HEDL Test HUT5-3A," Internal ANL/RAS Memorandum, August 1976.

7. G. S. Stanford, et al., "Fuel Motion in E8: Final Hodoscope Report," Internal ANL/RAS Memorandum, July 1976.

8. R. R. Stewart, et al., "Interium Report: Hodoscope Fuel Motion Analysis of TREAT In-Pile ANL/RAS Fuel Dynamics Loss-of-Flow Test L5-2," Internal ANL/RAS Memorandum, September 1976.

9. A. De Volpi et al., "Fast-Neutron Hodoscope at TREAT: Data Processing, Analysis, and Results," Nuclear Technology 30, 398-421 (1976).

10. A. De Volpi, "Material Motion Capabilities for SAREF," these Transactions.